Macromolecules
COMMUNICATION TO THE EDITOR

DOI: 10.1021/ma100449n

Dynamic Geometry and Kinetics of Polymer Confined in Self-Assembly via Cooperative Hydrogen Bonding: A Solid-State NMR Study under Paramagnetic Doping

Toshikazu Miyoshi,* Wei Hu, and Yongjin Li

Research Institute of Nanotechnology, National Institute of Advanced Industrial Science and Technology (AIST), Higashi 1-1-1 Tsukuba, Ibaraki 305-8565, Japan

Received February 28, 2010
Revised Manuscript Received April 19, 2010

Well-defined arrangements of the secondary intermolecular interactions play important roles for the design of new materials, which leads to unique self-assemblies consisting of multicomponent molecules with different sizes and shapes. Much work has gone into characterizing the static structures of such self-assembled systems.[1] Cooperative secondary interactions influence the molecular dynamics of the components and the bulk properties. Therefore, understanding relationship between microscopic dynamics and secondary interactions in self-assemblies is an important subject in this field.[2]

Poly(ethylene oxide) (PEO) is a hydrogen acceptor and can form supramolecular crystals with a small molecule of UREA, which is a hydrogen donor, in methanol solutions. XRD revealed that two-thirds of the UREA molecules form nanochannels with a diameter of ~1 nm, inside which isolated PEO chains and the remaining UREA molecules are included (Figure 1a).[3] Several groups have investigated PEO dynamics in this unique morphology by conventional NMR relaxation measurements and have suggested that the dynamics of PEO is restricted by cooperative hydrogen bonding.[4,5] However, the details of the geometry and kinetics of the molecular dynamics of PEO in this supramolecular system are not well understood.

Solid-state (SS) NMR techniques using magnetically anisotropic interactions can provide not only the kinetics and but also the geometry of the molecular dynamics.[6] In the past decade, various sophisticated SS-NMR techniques have been developed to investigate molecular dynamics in a wide frequency range in natural abundance.[7−11] Among them, center bands only detection of exchange (CODEX)[7,8] NMR can provide both the geometry and kinetics of molecular dynamics in a slow range and has been successfully applied to investigate the molecular dynamics of small molecules,[7] polymers,[12−14] liquid crystals,[15] and polymer blends.[16] However, this robust technique suffers from low NMR sensitivity, which has limited its application in chemically complex systems and/or systems with long T_{1H} values. Recently, Wickramasinghe et al. proposed a simple approach using paramagnetic doping for sensitivity enhancement.[17] Adding a small amount of a paramagnetic compound into a protein crystal could effectively shorten the T_{1H} value without disturbing the structures. Similar strategies may be applicable to self-assemblied systems. In this Communication, CODEX NMR and paramagnetic doping have been used to elucidate the dynamic nature of PEO in a PEO−UREA supramolecular system in natural abundance.

Figure 1a shows the ^{13}C CPMAS NMR spectrum for PEO-UREA supramolecules at 213 K and their structures. PEO shows a very sharp ^{13}C signal at 70 ppm. The single resonance supports

*To whom corresponding author should be addressed: e-mail t-miyoshi@aist.go.jp; Tel +81-298-61-9392; Fax +81-298-61-4437.

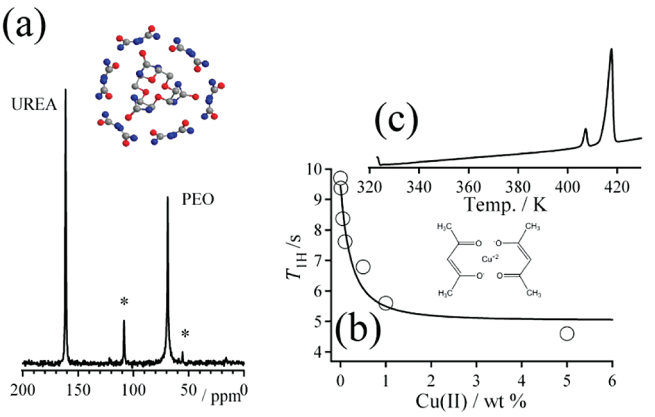

Figure 1. (a) ^{13}C CPMAS NMR spectrum for PEO−UREA supramolecular crystal at 213 K and the crystal structure determined by XRD.[3] (∗) Spinning-side bands. (b) The T_{1H} values of the supramolecules as a function of Cu(II)−AA wt % at an ambient temperature. (c) DSC heating scans of the supramolecular crystals after doping with Cu(II)−AA at 5 wt %.

the result the PEO chains adopt a uniform 4_1 helical conformation which was obtained by XRD.[3] The observed single resonance is in stark contrast to a bulk PEO signal, which has multiple splitting on its ^{13}C signal (Figure 2b). Using $^{13}C-^{13}C$ double quantum NMR combined with relaxation filters, Harris et al. concluded that the multiple splitting arose from different conformations and packing of disordered 7_2 helices in the crystalline region.[18] ^{14}N spins of UREA lead to relaxation-induced dipolar exchange with recoupling (RIEDER) effects[19] on spatially proximate ^{13}C spins. As a result, this effect may lead to undesired CODEX decay of the ^{13}C signal of PEO. To obtain CODEX decaying purely from molecular dynamics, ^{15}N-labeled UREA was utilized in this work. The ^{13}C CO signal of ^{15}N-labeled UREA shows a single resonance, which means that inner and outer UREA molecules cannot be distinguished using the ^{13}C chemical shift.

The supramolecular system shows a long T_{1H} value of 9.8 s at an ambient temperature. The long T_{1H} value is a drawback for further detailed dynamic analysis. PEO−UREA supramolecular crystals were formed from methanol solution. Bis(2,4-pentanedionato)Cu(II) (Cu(II)−AA), a paramagnetic compound, was added to the solution after the supramolecular particles had formed (see Supporting Information). This simple procedure easily allows for the attachment of Cu(II)−AA molecules to the particles. Figure 1b shows the T_{1H} value of the supramolecules as a function of Cu(II)−AA wt % relative to PEO weight used to make the supramolecules. At a low concentration, the T_{1H} value rapidly decreased with increasing Cu(II)−AA wt %. However, the T_{1H} value was almost saturated at concentrations higher than 1 wt % (T_{1H} = 4.8 s at 5 wt %). At 5 wt %, doping effects on local structure and thermal property were investigated. The ^{13}C line widths for PEO and UREA signals did not change with the doping. Additionally, DSC scan also showed the characteristic melting peak corresponding to the supramolecular crystals at 416 K,[20] with melting of some excess UREA crystals at 407 K (Figure 1c). These structural results and T_{1H} behaviors suggest that the Cu(II)−AA molecules simply attach to the surface and reduce the T_{1H} value due to a fast spin diffusion into the interior region without disturbing the bulk structures and thermal properties. Thus, CODEX NMR is achieved in half the experimental time.

Published on Web 04/22/2010

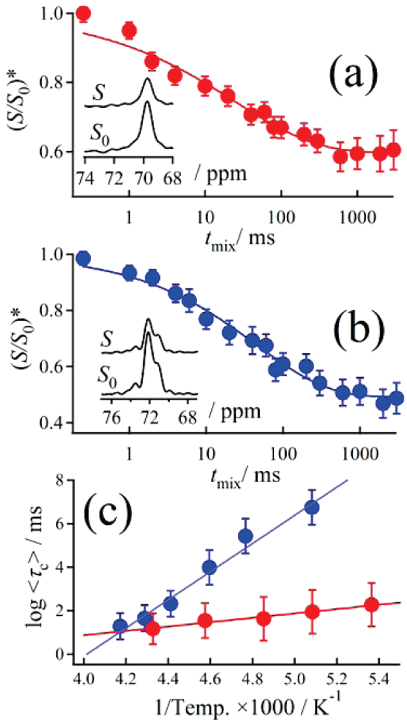

Figure 2. CODEX t_{mix} dependences of $(S/S_0)^*$ of (a) PEO in supramolecules at $Nt_r = 2.0$ ms at 218 K and (b) bulk PEO systems at $Nt_r = 1.5$ ms at 233 K and their exchange (S) and reference (S_0) spectra at $t_{mix} = 1$ s. The best fitted curves to the experimental data being shown as solid curves. The fitting equation being inserted into the text. (c) Arrhenius plot for $\langle\tau_c\rangle$ for PEO dynamics in supramolecules (red ●) and bulk crystals (blue ●). The solid curves showing best fitted E_a values of 19 ± 2 and 124 ± 9 kJ/mol for PEO in the supramolecules and bulk crystals, respectively.

Parts a and b of Figure 2 show mixing time, t_{mix} dependences of $(S/S_0)^*$ for PEO in the supramolecules at 218 K and bulk crystals at 233 K, respectively, where $(S/S_0)^*$ is the pure exchange decay after a spin-diffusion correction.[21] The CODEX exchange (S) and reference (S_0) spectra at $t_{mix} = 1$ s are shown as insets. A typical experiment for t_{mix} dependence using a 7 mm probe takes about 3 days for the supramolecules under paramagnetic doping (see Supporting Information). A series of t_{mix} data provide correlation time, $\langle\tau_c\rangle$, of the dynamics using the equation of $(S/S_0(t_{mix}))^* = 1 - a\exp(-(t_{mix}/\langle\tau_c\rangle)^{\beta})$, where a is related to the number of available sites (p) involved in the dynamic process by $a = (p-1)/p$, and β is the distribution width parameter, $0 < \beta \leq 1$. For the supramolecules, the curve of best fit on the experimental results gives $\langle\tau_c\rangle = 35 \pm 5$ ms, $a = 0.42 \pm 0.02$, and $\beta = 0.44 \pm 0.02$. These best-fit values are close to those in bulk PEO ($\langle\tau_c\rangle = 44 \pm 4$ ms, $a = 0.51 \pm 0.02$, and $\beta = 0.46 \pm 0.03$) obtained at 233 K. The same order of $\langle\tau_c\rangle$ of PEO in the supramolecules and bulk crystals is a direct evidence on retardation of PEO dynamics in supramolecules. Here, $\langle\tau_c\rangle$ for PEO dynamics in supramolecules and bulk crystals is further investigated over a wide temperature range. Figure 2c shows the Arrhenius plots of $\langle\tau_c\rangle$ obtained by CODEX experiments in both systems. The distribution width of the $\langle\tau_c\rangle$ values as converted from the β value is also shown as an error bar. Thermally activated process of $\langle\tau_c\rangle$ in PEO dynamics in the self-assembly is largely different from that of PEO in the bulk crystals. The activation energy, E_a, values for PEO dynamics in the supramolecules and bulk crystals are 19 ± 2 and 124 ± 9 kJ/mol, respectively. Before discussing a large difference in E_a values, the dynamic geometry of PEO was further investigated in both systems.

Figure 3a shows the evolution-time (Nt_r) dependence of (S/S_0) for PEO in the bulk crystals (blue ●) at 231 K, where N is an

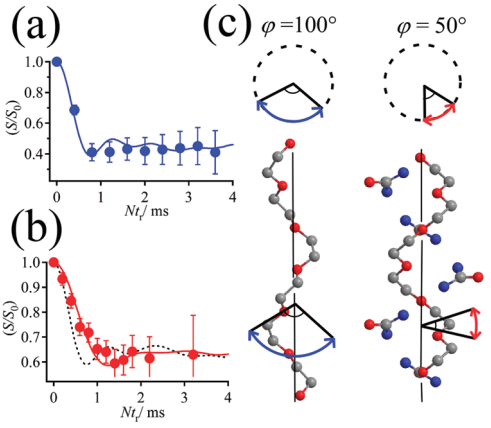

Figure 3. CODEX Nt_r dependence of (S/S_0) for PEO in (a) bulk (blue ●) and (b) supramolecular systems (red ●) at a $t_{mix} = 250$ ms at 231 and 240 K, respectively, and the simulated curves with jump angles of (a) 100 ± 20° (blue solid) for bulk PEO and (b) 50 ± 15° (red solid) for PEO in supramolecules. (c) Dynamic geometry of PEO in the bulk and supramolecular crystals as determined by CODEX NMR.

integer and t_r is a rotation period of MAS. The steepness of the decay curve of $(S/S_0(Nt_r))$ depends on the reorientaitonal angle and the principal values and orientations of the CSA tensor. The simulation was performed using literature values.[22] It has been shown by ^{13}C 2D exchange NMR that PEO in the bulk crystal performs helical jump motions around their axes.[6] We simulated CODEX results as a function of jump angle of entire chains around their axes. The simulated curve with a jump angle $\varphi = 100 \pm 20°$ gave the best fit for the experimental data as shown in Figure 3a. This jump angle is consistent with the reported reorientation angle for the helical jump motion of the PEO chains.

Figure 3b shows $(S/S_0(Nt_r))$ of PEO in the supramolecules. The result shows a slower initial decay than that in bulk PEO. This suggests that the dynamic geometry of PEO in supramolecules is more restricted than in bulk crystalline PEO. However, it is difficult to assign this to a proper dynamic mode using only the CODEX $((S/S_0(Nt_r))$ data. At $t_{mix} \gg \langle\tau_c\rangle$, $(S/S_0(t_{mix}))^*$ reaches to a plateau value, $(S/S_0)^*_{final}$, which is related to the site number by $(S/S_0)^*_{final} = 1/p$.[7] The experimentally obtained plateau value of 0.58 ± 0.02 at 218 K (Figure 2a) is close to 0.5, which is the value expected from a two-site jump motion. This result excludes diffusion type motions of the entire chains around their axes, which have been identified as primary modes in polymer dynamics in simple inclusion compounds.[23−26] The ^{13}C signal of PEO in the supramolecules shows only one resonance, even down to low temperature of 180 K. This experimental result exclude another possibility of conformational transitions.[27] Considering the structural constraints along the nanochannels and uniform conformation of PEO, a two-site helical jump of PEO entire chains about their axes is further investigated. Adopting the same tensor orientations of the CSA in PEO in the supramolecules as in the bulk PEO crystals, jump-angle effects on $(S/S_0(Nt_r))$ curves have been simulated. The best fit result with $\varphi = 50 \pm 15°$ to the experimental data is shown as a solid red curve in Figure 3b. These results evidently indicate that the jump angle of the PEO entire chains in the supramolecules is more restricted than in the bulk crystals (Figure 3c). In the latter, the chain conformations and their packing with neighboring chains govern their own dynamic geometry. Additionally, neighboring chains move concertedly. Such cooperative dynamics of chains with large amplitudes explain a high E_a value (124 kJ/mol). On the other hand, the geometry of PEO dynamics in the supramolecules is independent of its own conformations and is rather dominated by the periodic arrangement of interior UREA molecules along the chain axis.

Inner and outer UREA molecules isolate PEO chains and stabilize their conformations via cooperative hydrogen bonding. Therefore, the effects of (i) isolation of the PEO chains, (ii) cooperative hydrogen bonding, and (iii) space confinement due to inner UREA molecules result in a restricted two-site helical jump of the PEO chains with a low E_a value (19 kJ/mol).

In summary, paramagnetic doping was used to enhance the sensitivity of NMR for PEO−UREA self-assemblies without disturbing their structures and thermal properties. 1D-MAS exchange NMR with sensitivity enhancement was successfully applied to elucidate the effects of cooperative hydrogen bonding and confined spaces on the dynamic geometry and kinetics of PEO in self-assembled systems at natural abundance. This new strategy will be useful for other complex self-assemblies which are formed in solutions.

Acknowledgment. This work was financially supported by NEDO Nanostructure Polymer Project.

Supporting Information Available: Sample preparation, paramagnetic doping, and CODEX experiments. This material is available free of charge via the Internet at http://pubs.acs.org.

References and Notes

(1) Lawrence, D. S.; Jiang, T.; Levett, M. *Chem. Rev.* **1995**, *95*, 2229–2260.
(2) Brown, S. P.; Spiess, H. W. *Chem. Rev.* **2001**, *101*, 4125–4155.
(3) Chenite, A.; Brisse, F. *Macromolecules* **1991**, *24*, 2221–2225.
(4) Vasanthan, N.; Shin, I. D.; Tonelli, A. E. *Macromolecules* **1996**, *29*, 263–267.
(5) Hikichi, K.; Oka, D.; Shibata, T.; Uzawa, J. *Polym. J.* **1999**, *31*, 692–694.
(6) Schmidt-Rohr, K.; Spiess, H. W. *Multidimensional Solid-State NMR and Polymers*; Academic Press: London, 1994.
(7) deAzevedo, E. R.; Hu, W. G.; Bonagamba, T. J.; Schmidt-Rohr, K. *J. Am. Chem. Soc.* **1999**, *121*, 8411–8412.
(8) Reichert, D.; Pascui, O.; Bonagamba, T. J.; deAzevedo, E. R.; Schmidt, A. *Chem. Phys. Lett.* **2003**, *380*, 583–588.
(9) deAzevedo, E. R.; Saalwächter, K.; Pascui, O.; deSouza, A. A.; Bonagamba, T. J.; Reichert, D. *J. Chem. Phys.* **2008**, *128*, 104505-1–104505-12.
(10) Saalwächter, K.; Spiess, H. W. *J. Chem. Phys.* **2001**, *114*, 5707–5728.
(11) Liu, S. F.; Mao, J. D.; Schmidt-Rohr, K. *J. Magn. Reson.* **2002**, *155*, 15–28.
(12) Miyoshi, T.; Pascui, O.; Reichert, D. *Macromolecules* **2002**, *35*, 7178–7181.
(13) Bonagamba, T. J.; Becker-Guedes, F.; deAzevedo, E. R.; Schmidt-Rohr, K. *J. Polym. Sci., Part B: Polym. Phys.* **2001**, *39*, 2444–2453.
(14) Miyoshi, T.; Mamun, A.; Hu, W. *J. Phys. Chem. B* **2010**, *114*, 92–100.
(15) Fishbach, I.; Pakula, T.; Minkin, P.; Fechtenkötter, A.; Müllen, K.; Spiess, H. W.; Saalwächter, K. *J. Phys. Chem. B* **2002**, *106*, 6408–6418.
(16) Wachowicz, M.; White, J. L. *Macromolecules* **2007**, *40*, 5433–5440.
(17) Wickramasinghe, N. P.; Kotecha, M.; Samoson, A.; Past, J.; Ishii, Y. *J. Magn. Reson.* **2007**, *184*, 350–356.
(18) Harris, D. J.; Bonagamba, T. J.; Hong, M.; Schmidt-Rohr, K. *Polymer* **2005**, *46*, 11737–11743.
(19) Saalwächter, K.; Schmidt-Rohr, K. *J. Magn. Reson.* **2000**, *145*, 161–172.
(20) Liu, Y.; Pellerin, C. *Polymer* **2009**, *50*, 2601–2607.
(21) Pascui, O.; Beiner, M.; Reichert, D. *Macromolecules* **2003**, *36*, 3992–4003.
(22) Schmidt-Rohr, K.; Wilhelm, M.; Johansson, A.; Spiess, H. W. *Magn. Reson. Chem.* **1993**, *31*, 352–356.
(23) Lu, J.; Mirau, P. A.; Tonelli, A. E. *Prog. Polym. Sci.* **2002**, *27*, 357–401.
(24) Saalwächter, K. *Macromol. Rapid Commun.* **2002**, *23*, 286–291.
(25) Sozzani, P.; Comotti, A.; Bracco, S.; Simonutti, R. *Chem. Commun.* **2004**, *7*, 768–769.
(26) Zhan, Y.; Mattice, W. L. *Macromolecules* **1992**, *25*, 4078–4083.
(27) Giraadeau, T. E.; Leisen, J.; Beckham, H. W. *Macromol. Chem. Phys.* **2005**, *206*, 998–1005.